

Article

Imidazopyranotacrines as Non-Hepatotoxic, Selective Acetylcholinesterase Inhibitors, and Antioxidant Agents for Alzheimer's Disease Therapy

Housseem Boulebd¹, Lhassane Ismaili^{2,*}, Manuela Bartolini³, Abdelmalek Bouraiou¹, Vincenza Andrisano⁴, Helene Martin⁵, Alexandre Bonet⁵, Ignacio Moraleda⁶, Isabel Iriepa⁶, Mourad Chioua⁷, Ali Belfaitah^{1,*} and José Marco-Contelles^{7,*}

¹ Equipe de Synthèse de Molécules à Objectif Thérapeutique, Laboratoire des Produits Naturels d'Origine Végétale et de Synthèse Organique (PHYSYNOR), Université des frères Mentouri, Campus de Chaabat-Ersas, Constantine 25000, Algeria; boulebdhousseam@hotmail.fr (H.B.); bouraiou.abdelmalek@yahoo.fr (A.B.)

² Laboratoire de Chimie Organique et Thérapeutique, Neurosciences Intégratives et Cliniques EA 481, UFR SMP, Univ. Franche-Comté, Univ. Bourgogne Franche-Comté, 19, rue Ambroise Paré, F-Besançon 25000, France

³ Department of Pharmacy and Biotechnology, University of Bologna, Via Belmeloro 6, Bologna 40126, Italy; manuela.bartolini3@unibo.it

⁴ Department for Life Quality Studies, University of Bologna, Corso d'Augusto, 237, Rimini 47921, Italy; vincenza.andrisano@unibo.it

⁵ Laboratoire de Toxicologie Cellulaire, EA 4267, Univ. Bourgogne Franche-Comté, 19, rue Ambroise Paré, Besançon Cedex 25030, France; helene.martin@univ-fcomte.fr (H.M.); alexandre.bonet@univ-fcomte.fr (A.B.)

⁶ Departamento de Química Orgánica y Química Inorgánica, Facultad de Biología, Ciencias Ambientales y Química, Universidad de Alcalá, Ctra. Barcelona, Km. 33.5, Alcalá de Henares 28817, Spain; ignacio.moraleda@uah.es (I.M.); isabel.iriapa@uah.es (I.I.)

⁷ Laboratory of Medicinal Chemistry (IQOG, CSIC), C/Juan de la Cierva 3, Madrid 28006, Spain; mchioua@gmail.com

* Correspondence: lhassane.ismaili@univ-fcomte.fr (L.I.); abelbelfaitah@yahoo.fr (A.B.); iqoc21@iqog.csic.es (J.M.-C.); Tel.: +33-381-665-543 (L.I.); +21-331-111-113 (A.B.); +34-915-622-900 (J.M.-C.); Fax: +33-363-082-319 (L.I.); +21-331-111-113 (A.B.); +34-564-4853 (J.M.-C.)

Academic Editors: Michael Decker and Diego Muñoz-Torrero

Received: 27 January 2016 ; Accepted: 15 March 2016 ; Published: 24 March 2016

Abstract: Herein we describe the synthesis and *in vitro* biological evaluation of thirteen new, racemic, diversely functionalized *imidazo pyranotacrines* as non-hepatotoxic, multipotent tacrine analogues. Among these compounds, 1-(5-amino-2-methyl-4-(1-methyl-1*H*-imidazol-2-yl)-6,7,8,9-tetrahydro-4*H*-pyrano[2,3-*b*]quinolin-3-yl)ethan-1-one (**4**) is non-hepatotoxic (cell viability assay on HepG2 cells), a selective but moderately potent *EeAChE* inhibitor ($IC_{50} = 38.7 \pm 1.7 \mu M$), and a very potent antioxidant agent on the basis of the ORAC test ($2.31 \pm 0.29 \mu mol \cdot Trolox / \mu mol$ compound).

Keywords: tacrine analogues; hepatotoxicity; cholinesterase inhibitors; antioxidant activity; ORAC; Alzheimer's disease

1. Introduction

Alzheimer's disease (AD) is an age-related neurodegenerative disorder whose prevalence is expected to rise significantly in the next decades as the average age of the population increases [1]. Worldwide, around 40 million people suffer from AD [2], which is characterized by a progressive memory loss, a decline in language skills and motor capabilities along with other cognitive impairments [3]. Although the etiology of AD is not completely known, common hallmarks such as β -amyloid ($A\beta$) deposits [4], τ -protein aggregation [5] and oxidative stress [6] play key roles in the

physiopathology of the disease [7]. In addition, the selective loss of cholinergic neurons in AD results in a deficit of the neurotransmitter acetylcholine (ACh) in specific brain regions that mediate learning and memory [8]. Alterations in the serotonergic and dopaminergic systems are also thought to be responsible for the behavioral disturbances observed in AD patients [9]. At present, there are three FDA-approved drugs (donepezil, galantamine and rivastigmine) [10] that ameliorate AD symptoms by inhibiting acetylcholinesterase (AChE), the enzyme responsible for the hydrolysis of ACh, and by rising the ACh content in the synapsis [11]. Apart from the beneficial palliative properties of AChE inhibitors (AChEI) in AD, cholinergic drugs have shown little efficacy to prevent the progression of the disease. Consequently, nowadays there is no efficient therapy to cure, stop or even slow the progression of the disease. Hence, effective therapeutics are urgently sought [12].

The failure to find such a drug or treatment is possibly due to the multifactorial nature of AD. Thus, single drugs acting on specific targets to produce the expected clinical effects might not be effective in interfering with the complex nature of AD. This is the reason why the multi-target-directed ligand (MTDL) approach [13] has received an increasing attention by many research groups that have developed a variety of compounds binding very diverse biochemical targets [14].

Among the AChEIs investigated in the search for a pharmacological treatment for AD, the case of tacrine is particularly relevant [15]. Tacrine (Figure 1) is one of the strongest butyrylcholinesterase (BuChE) inhibitors known to date [16]. This drug, which was withdrawn from the clinical use for AD treatment because of significant liver toxicity [17], has been largely stigmatized instead of being further developed looking for other non-toxic tacrines retaining valuable anti-ChE properties [18]. In this context, we have reconsidered tacrine as a starting scaffold in the design of new Multipotent Non-Toxic Tacrines (MNTTs), [19] by incorporating other pharmacophoric groups capable of binding or inhibiting other molecular targets involved in the onset and/or progression of the disease. With this idea in mind, since 1997 we developed different types of structurally simple and easily available MNTTs [20].

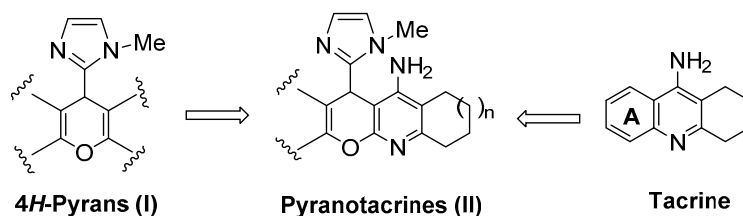


Figure 1. General structure of tacrine, 4*H*-pyrans (I), and the new racemic *imidazopyranotacrines* (II).

Thus, expanding our contribution in this area, in this work we report the synthesis of a number of new *imidazopyranotacrines* (II), a new family of tacrine derivatives resulting from the substitution of the ring A in tacrine by the 4*H*-pyrano (I) heterocyclic motif (Figure 1). In this case, we have incorporated, and at the same position, instead of a substituted phenyl ring [21], or a five- (furan [22], thiophen [22], pyrrole [22]) or six-membered heterocyclic ring system [23], the five-membered 1-methyl-1*H*-imidazol-2-yl motif, in order to improve previous biological results and gain new insights on the structure-activity relationship (SAR) of pyranotacrines. The imidazole ring is a privileged heterocyclic ring system [24] which is present in a number of interesting biologically active molecules such as saripidem, necopidem or zolpidem [25]. This choice was also favored by the ready availability of the imidazole substituted starting derivatives.

Thus, in this work, we describe the synthesis and biological evaluation of the new *imidazopyranotacrines* 1–13 (Figure 2), the inhibition of AChE and BuChE enzymes, the antioxidant activities (ORAC-FL method), as well as the evaluation of their hepatotoxicity on HepG2 cells. As a result, we have identified racemic 1-(5-amino-2-methyl-4-(1-methyl-1*H*-imidazol-2-yl)-6,7,8,9-tetrahydro-4*H*-pyrano[2,3-*b*]quinolin-3-yl)ethan-1-one (4) (Figure 2) as a non-hepatotoxic compound

on HepG2 cells, endowed with selective but moderate inhibitory activity against AChE from *Electrophorus electricus* (EeAChE), and very potent antioxidant activity.

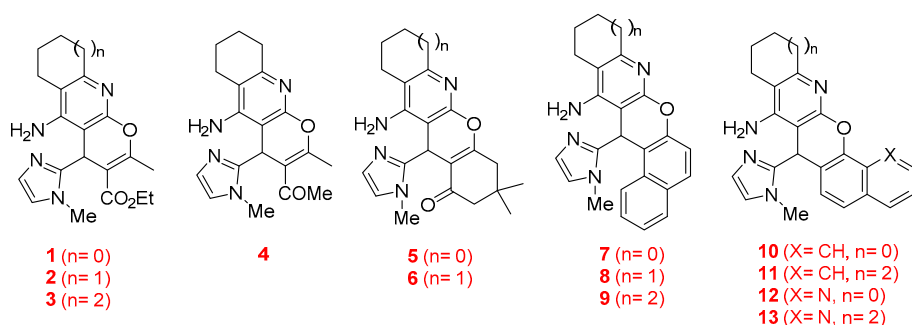
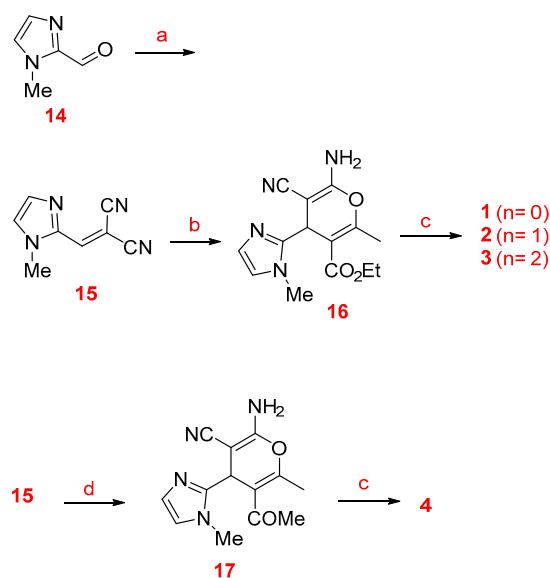


Figure 2. Structures of the *imidazopyranotacrines* 1–13.

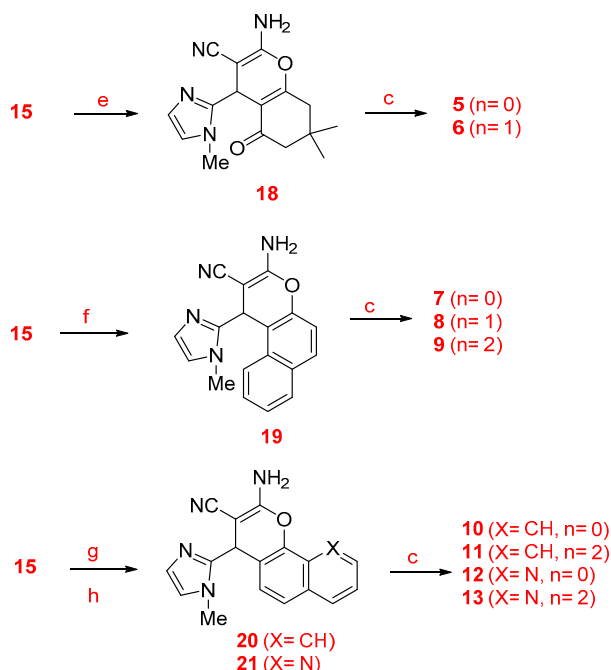
2. Results and Discussion

2.1. Chemistry

The synthesis of racemic *imidazopyranotacrines* 1–13 has been carried out by Friedländer-type reactions [26], by treating readily available 4*H*-pyrans with commercial cycloalkanones, under standard reaction conditions, and in good chemical yields. Cyclopentanone, cyclohexanone and cycloheptanone were chosen in order to evaluate the effect of the size of the cycloalkyl ring on the biological activity of the new pyranotacrines (Scheme 1). Starting from 1-methyl-1*H*-imidazole-2-carbaldehyde (**14**), we synthesized 2-(1-methyl-1*H*-imidazol-2-yl)methylene)malononitrile (**15**), whose reaction with the appropriate 1,3-dicarbonylic compound or naphthol derivative, gave the key 4*H*-pyrans. For the synthesis of pyranotacrines 1–3, we have used ethyl acetoacetate as starting material, thus leading to *imidazopyranotacrines* bearing a methyl and ethoxycarbonyl substituents at C-2 and C-3, respectively. Similarly, for the synthesis of the pyranotacrines **4** and **5** or **6**, we used 2,4-pentandione, and 5,5-dimethylcyclohexane-1,3-dione, respectively. Finally, for the synthesis of the remaining pyranotacrines **19**–**21** we have prepared some conveniently key functionalized 4*H*-pyrans from 1-naphthol, 2-naphthol, and 8-hydroxyquinoline. All new compounds showed excellent analytical and spectroscopic data, in good agreement with their structures.



Scheme 1. Cont.



Scheme 1. Synthesis of the *imidazopyranotacrines* 1–13. *Reagents and conditions:* (a) Malononitrile, piperidine, ethanol, rt (93%); (b) ethyl 3-oxobutanoate, piperidine, ethanol, rt (92%); (c) cyclopentanone ($n = 0$), cyclohexanone ($n = 1$), cycloheptanone ($n = 2$), AlCl_3 , 1,2-dichloroethane, reflux; (d) pentane-2,4-dione, piperidine, ethanol, rt (90%); (e) 5,5-dimethylcyclohexane-1,3-dione, piperidine, ethanol, rt (69%); (f) 2-naphthol, piperidine, ethanol, rt (72%); (g) 1-naphthol, piperidine, ethanol, rt (75%); (h) 8-hydroxyquinoline, piperidine, ethanol, rt (47%).

2.2. Biological Assays

2.2.1. Inhibition of the Cholinesterase Enzymes and Kinetic Analysis

First of all, we addressed the capacity of *imidazopyranotacrines* 1–13 to inhibit *EeAChE* and serum horse BuChE (*eqBuChE*) by using Ellman's assay [27], and tacrine as reference compound for comparative purposes [28].

As shown in Table 1, racemic *imidazopyranotacrines* 1–13 were very modest *EeAChE* inhibitors with potencies in the micromolar range, resulting from two to three orders of magnitude less active than the reference compound tacrine. On the other hand, all derivatives acted as highly selective AChEI, as no or very moderate inhibition of *eqBuChE* activity was observed. The most potent *EeAChEI* was the *imidazopyranotacrine* 8 ($\text{IC}_{50} = 6.73 \pm 0.52 \mu\text{M}$), followed, in decreasing order of activity, by 7, 10, 2 and 1. The three most potent *EeAChE*s among the *imidazopyranotacrines* (*i.e.*, 8, 7 and 10) bear a naphthol ring fused to the central 4*H*-pyran motif. Furthermore, the 2-naphthol derivatives (7, 8) were more potent than the 1-naphthol ones (10, 11). The 2-naphthol derivative bearing a cyclohexane ring (8) is more potent than the analogues bearing a cyclopentane motif (7) or a cycloheptane motif (9). Note that the incorporation of a heterocyclic nitrogen in the 1-naphthol compounds (compare compound 11 with 13) significantly potentiates the inhibition of *EeAChE*, affording additional capacity for the inhibition of *eqBuChE*. For the other *imidazopyranotacrines*, it is clear that those bearing an ethoxycarbonyl moiety and a methyl group at C3 and C2, respectively, in the 4*H*-pyran core (1, 2) are more potent than those bearing a fused 3,3-dimethylcyclohexan-1-one (6, 5) or an acetyl and a methyl group (4) at C3 and C2, respectively, in the 4*H*-pyran core. Note also that *imidazopyranotacrines* 1 and 2, differing only in the size of the cycloalkyl ring, are almost equipotent *EeAChE*s, while 3, bearing a cycloheptane ring, is two orders of magnitude less active. Finally, regarding *eqBuChE* inhibition, *imidazopyranotacrines* 1–13 were very weak BuChEIs. Because of the weak inhibitory activity, high concentrations were

required for the determination of the IC₅₀ values, exceeding the solubility of some compounds. Thus, imidazopyranotacrines 1–13 were screened at a single concentration, namely 10 μM, giving percentages of inhibition between 12.9 and 75.7 (Table 1).

Table 1. Inhibitory potencies, expressed as IC₅₀ values (μM), for the inhibition of *EeAChE* and *eqBuChE*, and antioxidant power of imidazopyranotacrines 1–13.

Compound	<i>EeAChE</i> ^a IC ₅₀ Values (μM)	<i>eqBuChE</i> ^b % Inhibition at 10 μM	ORAC ^d
1	12.9 ± 0.3	25.6 ± 0.7	0.34 ± 0.03
2	11.5 ± 0.4	34.0 ± 0.5	1.79 ± 0.17
3	432 ± 84	32.2 ± 0.9	1.99 ± 0.23
4	38.7 ± 1.7	24.9 ± 0.9	2.31 ± 0.29
5	158 ± 33	12.9 ± 0.5	1.70 ± 0.33
6	37.8 ± 1.2	33.5 ± 1.7	2.34 ± 0.31
7	8.41 ± 0.14	50.5 ± 7.3	1.47 ± 0.13
8	6.73 ± 0.52	51.6 ± 0.6	1.88 ± 0.01
9	na	15.1 ± 4.7	1.35 ± 0.13
10	10.7 ± 0.2	25.0 ± 0.2	2.75 ± 0.09
11	na	20.3 ± 3.7	2.33 ± 0.13
12	15.3 ± 0.6	27.5 ± 1.1	1.88 ± 0.07
13	30.0 ± 2.0	75.7 ± 2.3	2.25 ± 0.29
Tacrine	0.0898 ± 0.0022	0.005 ± 0.001 ^{a,c}	0.20 ± 0.04 [28]

^a Each IC₅₀ value is the mean ± SEM of at least two independent experiments each performed in triplicate.

^b % inhibition at 10 μM is the mean ± SEM of at least three independent experiments. ^c IC₅₀ value of tacrine was given. ^d Data expressed as μmol Trolox/μmol compound. na: not significantly active (% inhibition lower than 15%) when tested at the highest concentration (solubility limit), namely 15 μM and 25 μM for 9 and 11, respectively.

The mechanism of inhibition of *EeAChE* by the most potent AChEI, imidazopyranotacrine 8, was investigated by building Lineweaver-Burk double reciprocal plots at increasing concentrations of inhibitor and substrate (acetylthiocholine). Analysis of the Lineweaver-Burk reciprocal plots (Figure 3A) showed that K_m appeared unaltered while V_{max} decreased at increasing concentrations of the inhibitor. This pattern indicated that 8 acts as a non-competitive enzyme inhibitor. The non-competitive mechanism of action was confirmed by building the Cornish-Bowden plot (Figure 3B). Replots of the substrate/velocity versus the concentration of compound 8 provided an estimate of the non-competitive inhibition constant [29], which resulted equal to 4.10 μM. The non-competitive mechanism of action was confirmed by computational chemistry by performing the docking analysis of both enantiomers of compound 8 on AChE (see Supplementary Materials).

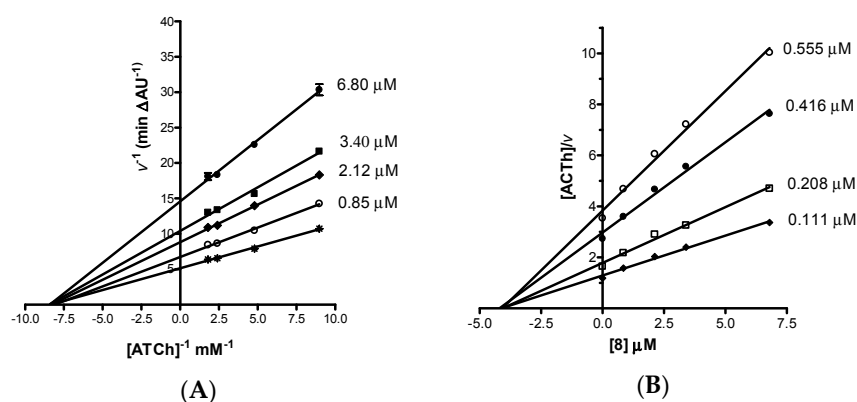


Figure 3. (A) Lineweaver-Burk plot and (B) Cornish-Bowden plot both illustrating non-competitive inhibition of *EeAChE* by compound 8. The intersection point in Cornish-Bowden plot gives an estimate of the inhibition constant. Lines were derived from a weighted least-squares analysis of data. ATCh = acetylthiocholine (substrate).

2.2.2. Antioxidant Power

The antioxidant power of the *imidazopyranotacrines* 1–13 was determined by the oxygen radical absorbance capacity by fluorescence (ORAC-FL) method [30] using fluorescein as fluorescent probe and Trolox (6-hydroxy-2,5,7,8-tetramethylchroman-2-carboxylic acid) as a reference compound. Results are expressed as Trolox equivalents (μmol Trolox per μmol test compound). As shown in Table 1, all the *imidazopyranotacrines* were able to reduce the amount of peroxy radical, with ORAC values ranging from 1.35 (9) to 2.75 (10). The most potent antioxidant agent was 10 (2.75), followed by 6 (2.34), 11 (2.33), 4 (2.31) and 13 (2.25). Although it was clear that the naphthol derivatives, and particularly the 1-naphthol derivatives 10 and 13, were very potent, we observed that compounds 6 and 4, bearing a fused 3,3-dimethylcyclohexan-1-one, or an acetyl and a methyl groups at C3 and C2, respectively, in the 4*H*-pyran core, also showed high antioxidant power. Note also that tacrine has a very low ORAC value (0.20 ± 0.04) [28] compared with most of our synthetic *imidazopyranotacrines*.

Next, and on the basis of the AChE inhibition and ORAC values, *imidazopyranotacrines* 2, 4, 8 and 10 were evaluated for their potential hepatotoxicity, since tacrine was withdrawn from the market because of its liver toxicity.

2.2.3. Hepatotoxicity Analysis on HepG2 Cells

Drug-induced hepatotoxicity is one of the major reasons for drug [31] withdrawal from the clinic [15], as it happened to tacrine. HepG2 cell is a well-known *in vitro* system to screen the hepatotoxicity activity [32]. As shown in Table 2, tacrine was safe up to 100 μM , but significantly decreased cell viability at 300 μM and at higher concentrations. Among the selected derivatives, compounds 10 and 8 were more toxic than tacrine (significant reduction of cell viability at 30 and 100 μM), *imidazopyranotacrines* 2 and 4 resulted significantly less hepatotoxic than tacrine, and very interestingly, were safe even at 300 μM . *Imidazopyranotacrine* 4 showed the best safety profile, and proved to be non-toxic even at the highest tested concentration, namely 1000 μM , with a recorded cell viability value not significantly different from the control (not significant by the ANOVA test).

Table 2. *In vitro* toxicity of *imidazopyranotacrines*, and tacrine in HepG2 cells.

Compounds	1 μM	3 μM	10 μM	30 μM	100 μM	300 μM	1000 μM
Tacrine	95.8 \pm 2.2	100.4 \pm 2.2	96.9 \pm 3.9	97.7 \pm 3.9	98.6 \pm 3.8	39.2 \pm 4.7 ***	20.0 \pm 2.1 ***
10	101.8 \pm 4.2	100.7 \pm 2.6	100.5 \pm 1.9	71.4 \pm 7.4 *	63.5 \pm 6.2 *	64.8 \pm 5.7 *	66.8 \pm 4.1 *
8	108.1 \pm 5.4	101.3 \pm 10.8	79.0 \pm 9.1	57.6 \pm 4.2 **	52.7 \pm 3.3 **	51.2 \pm 2.8 **	66.2 \pm 6.8 *
2	102.7 \pm 3.7	103.2 \pm 4.4	101.3 \pm 3.9	99.2 \pm 2.6	93.0 \pm 4.7	87.5 \pm 3.2	58.8 \pm 2.1 *
4	107.7 \pm 5.1	105.3 \pm 2.9	102.1 \pm 2.9	98.0 \pm 3.1	104.6 \pm 4.5	97.1 \pm 3.0	96.8 \pm 1.5

Cell viability was measured as MTT reduction and data were normalized as % control. Data are expressed as the mean \pm S.E.M. of triplicate of at least three different cultures. All compounds were assayed at increasing concentrations (1–1000 μM). *** $p \leq 0.001$, ** $p \leq 0.01$, * $p \leq 0.05$, with respect to control group. Comparisons between tested compounds and control group were performed by one-way ANOVA.

3. Materials and Methods

3.1. General Information

Melting points were determined on a Kofler apparatus, and are uncorrected. IR spectra were recorded on a Shimadzu FT-IR 8201 PC spectrophotometer (Shimadzu, Kyoto, Japan), and only significant absorption bands are reported. $^1\text{H-NMR}$ and $^{13}\text{C-NMR}$ spectra were recorded on a Bruker Avance DPX250 (Bruker Avance DPX250, Bruker BioSpin, Fällanden, Switzerland) or VARIAN Mercury-300 (Palo Alto, CA, USA) spectrometers at 250 or 300 MHz and at 62 or 75 MHz, respectively in CDCl_3 , $\text{DMSO-}d_6$ or CD_3CN at 250 or 300 MHz and at 62 or 75 MHz, respectively, using solvent peaks as internal reference. Elemental analyses were performed on a Carlo-Erba CHNS apparatus, at CNQO (Madrid, Spain). TLC were performed on precoated Merck (Kenilworth, NJ, USA) silica gel aluminum sheets 60 F254 and detection by UV light at 254 nm or by charring with either ninhydrin,

anisaldehyde or phosphomolybdic-H₂SO₄ reagents. Anhydrous solvents were used in all experiments. Flash column chromatography was performed on silica gel 60 (230 mesh). Commercial grade reagents were used as supplied from Acros (Geel, Belgium) or Aldrich (Saint Louis, MO, USA).

3.2. General Procedure for the Preparation of 1-Methylimidazole-4H-pyran Derivatives

To a solution of the 2-(1-methyl-1H-imidazol-2-yl)methylene)malononitrile (**15**) in ethanol (1 mmol/10 mL), the corresponding 1,3-dicarbonyl (1.1 mmol), and some drops of piperidine were added. The mixture was stirred at room temperature (rt) and the reaction was monitored by TLC. The precipitated solid was isolated by filtration, washed with cold ethanol, and purified by silica gel flash chromatography using AcOEt/Hexane (1:1) as eluent to give pure compounds.

3.3. General Procedure for the Preparation of 1-Methylimidazole-4H-pyran Derivatives from 1- or 2-Naphthol

A mixture of 1 mmol of 2-((1-methyl-1H-(benz)imidazol-2-yl) methylene)malononitrile and 1- or 2-naphthol (1 mmol) in ethanol (10 mL) containing 2–3 drops of piperidine was heated under reflux for overnight. The reaction mixture was cooled and the precipitated product filtered, washed with cold ethanol and purified by silica gel flash chromatography using AcOEt or acetone as eluent to give pure compounds.

3.4. General Method for the Friedländer Reaction

Aluminum chloride (1.5 equiv) was suspended in dry 1,2-dichloroethane at rt. Then, the 4H-pyran (1 equiv) and the selected cycloalkanone (1.5 equiv) were added, and the reaction mixture was heated at reflux for 24 h. When the reaction was over (thin layer chromatography analysis), an aqueous solution of sodium hydroxide (10%) was added dropwise to the mixture until the aqueous solution became basic. After stirring for 30 min, the precipitate was filtered off and washed with water. The resultant solid was purified by silica gel flash chromatography using AcOEt as eluent to give pure compounds.

2-(1-Methyl-1H-imidazol-2-yl)methylene)malononitrile (15). To a solution of 1-methyl-1H-imidazole-2-carbaldehyde (**14**) in ethanol (1.1 g, 10 mmol), 1 equiv (1.58 g, 10 mmol) of malononitrile and 2–3 drops of piperidine were added, and the mixture was stirred at rt overnight. The precipitated product was filtered off and washed with cold ethanol to afford 1.47 g (9.3 mmol) of 2-(1-methyl-1H-imidazol-2-yl)methylene)malononitrile (**15**) (93% yield): mp 200–202 °C; IR (KBr) ν_{\max} 2210 (CN) cm^{-1} ; ¹H-NMR (250 MHz, DMSO-*d*₆) δ 8.15 (s, 1H), 7.58 (s, 1H), 7.40 (s, 1H), 3.79 (s, 3H); ¹³C-NMR (62.9 MHz, CD₃CN) δ 142.7, 141.1, 134.0, 129.2, 115.8, 114.1, 79.3, 34.1. Anal. Calcd. for C₈H₆N₄: C, 60.75; H, 3.82; N, 35.42. Found: C, 60.50; H, 4.03; N, 35.61.

Ethyl 6-amino-5-cyano-2-methyl-4-(1-methyl-1H-imidazol-2-yl)-4H-pyran-3-carboxylate (16). According to the general procedure, 2-(1-methyl-1H-imidazol-2-yl)methylene)malononitrile (**15**) (160 mg, 1.01 mmol), ethyl acetoacetate (150 mg, 1.15 mmol), and piperidine (2–3 drops), gave 270 mg (0.93 mmol) of the title compound **16** (93% yield): mp 230 °C; IR (KBr) ν_{\max} 3390 (NH₂), 2318 (CN), 1689 (CO) cm^{-1} ; ¹H-NMR (300 MHz, DMSO-*d*₆) δ 6.96–6.94 (m, 3H), 6.69 (s, 1H), 4.59 (s, 1H), 3.99–3.87 (m, 2H), 3.65 (s, 3H), 2.30 (s, 3H), 0.97 (t, *J* = 7.1 Hz, 3H); ¹³C-NMR (74.5 MHz, DMSO-*d*₆) δ 165.2, 158.7, 157.6, 149.6, 126.6, 120.7, 119.8, 105.0, 60.0, 54.5, 32.1, 30.1, 18.2, 13.8. Anal. Calcd. for C₁₄H₁₆N₄O₃: C, 58.32; H, 5.59; N, 19.43. Found: C, 58.09; H, 5.49; N, 19.32.

5-Acetyl-2-amino-6-methyl-4-(1-methyl-1H-imidazol-2-yl)-4H-pyran-3-carbonitrile (17). In the same manner, 2-(1-methyl-1H-imidazol-2-yl)methylene)malononitrile (**15**) (160 mg, 1.01 mmol), 2,4-pentadione (115 mg, 1.15 mmol), and piperidine (2–3 drops), gave 230 mg (0.89 mmol) of the title compound **17** (90% yield): mp 220 °C; IR (KBr) ν_{\max} 3394 (NH₂), 2218 (CN), 1616 (CO) cm^{-1} ; ¹H-NMR (300 MHz, DMSO-*d*₆) δ 7.00–6.96 (s, 3H), 6.71 (s, 1H), 4.76 (s, 1H), 3.66 (s, 3H), 2.32 (s, 3H), 2.01 (s, 3H); ¹³C-NMR (74.5 MHz, DMSO-*d*₆) δ 197.5, 159.0, 155.9, 148.8, 126.7, 121.6, 119.9, 113.2, 54.2, 32.3, 30.9, 29.6, 18.8. Anal. Calcd. for C₁₃H₁₄N₄O₂: C, 60.45; H, 5.46; N, 21.69. Found: C, 60.23; H, 5.42; N, 21.55.

2-Amino-7,7-dimethyl-4-(1-methyl-1H-imidazol-2-yl)-5-oxo-5,6,7,8-tetrahydro-4H-chromene-3-carbonitrile (18). 2-(1-Methyl-1H-imidazol-2-yl)methylene)malononitrile (**15**) (160 mg, 1.01 mmol), dimedone (155 mg, 1.1 mmol) and piperidine (2–3 drops), gave 205 mg (0.69 mmol) of the title compound **18** (69% yield): mp 192–193 °C; IR (KBr) \max 3367 (NH₂), 2183 (CN), 1689 (CO) cm⁻¹; ¹H-NMR (300 MHz, DMSO-*d*₆) δ 7.01 (s, 2H), 6.92 (s, 1H), 6.66 (s, 1H), 4.44 (s, 1H), 3.70 (s, 3H), 2.56–2.03 (m, 4H), 1.03 (s, 3H), 0.99 (s, 3H); ¹³C-NMR (74.5 MHz, DMSO-*d*₆) δ 196.0, 162.6, 158.9, 149.3, 126.5, 120.6, 119.9, 111.3, 55.5, 49.8, 32.3, 32.1, 25.5, 26.9, 26.5. Anal. Calcd. for C₁₆H₁₈N₄O₂: C, 64.41; H, 6.08; N, 18.78. Found: C, 64.50; H, 6.02; N, 18.94.

2-Amino-4-(1-methyl-1H-imidazol-2-yl)-4H-benzo[h]chromene-3-carbonitrile (20). According to the general procedure, 2-(1-methyl-1H-imidazol-2-yl)methylene)malononitrile (**15**) (160 mg, 1.01 mmol), 1-naphthol (146 mg, 1.01 mmol) and piperidine (2–3 drops), gave 228 mg (0.75 mmol) of the title compound **20** (75% yield): mp > 260 °C; IR (KBr) \max 3433 (NH₂), 2376 (CN) cm⁻¹; ¹H-NMR (250 MHz, CD₃CN) δ 7.95–7.90 (m, 2H), 7.78–7.75 (m, 1H), 7.53–7.43 (m, 2H), 7.30 (d, *J* = 8.91 Hz, 1H), 7.15 (br,s, 2H), 7.98 (s, 1H), 6.67 (s, 1H), 5.56 (s, 1H), 3.65 (s, 3H); ¹³C-NMR (62.9 MHz, CD₃CN) δ 160.4, 148.9, 146.8, 130.7, 130.6, 129.8, 128.5, 127.3, 126.6, 125.1, 123.2, 121.9, 120.5, 116.8, 113.1, 53.7, 32.4, 31.5. Anal. Calcd. for C₁₈H₁₄N₄O: C, 71.51; H, 4.67; N, 18.53. Found: C, 71.38; H, 4.51; N, 18.46.

2-Amino-1-(1-methyl-1H-imidazol-2-yl)-1H-benzof[f]chromene-3-carbonitrile (19). Following the same procedure, 2-(1-methyl-1H-imidazol-2-yl)methylene)malononitrile (**15**) (160 mg, 1.01 mmol), 2-naphthol (146 mg, 1.01 mmol) and piperidine (2–3 drops), gave 218 mg (0.72 mmol) of the title compound **19** (72% yield): mp > 260 °C; IR (KBr) \max 3440 (NH₂), 2183 (CN) cm⁻¹; ¹H-NMR (250 MHz, DMSO-*d*₆) δ 7.96–7.92 (m, 2H), 7.78–7.75 (m, 1H), 7.51–7.43 (m, 2H), 7.30 (d, *J* = 8.9 Hz, 2H), 6.99 (d, *J* = 0.8 Hz, 1H), 6.67 (d, *J* = 0.9 Hz, 1H), 5.67 (s, 1H), 3.66 (s, 3H); ¹³C-NMR (62.9 MHz, DMSO-*d*₆) δ 160.4, 148.9, 146.8, 130.7, 130.4, 129.7, 128.5, 127.3, 126.6, 125.0, 123.2, 121.9, 120.5, 116.8, 113.1, 53.7, 32.4, 31.4. Anal. Calcd. for C₁₈H₁₄N₄O: C, 71.51; H, 4.67; N, 18.53. Found: C, 71.47; H, 4.50; N, 18.72.

*2-Amino-4-(1-methyl-1H-imidazol-2-yl)-4H-pyranol[3,2-*h*]quinoline-3-carbonitrile (21)*. Using the procedure described above, 2-(1-methyl-1H-imidazol-2-yl)methylene)malononitrile (**15**) (160 mg, 1.01 mmol), 8-hydroxyquinoline (147 mg, 1.01 mmol) and piperidine (2–3 drops), gave 142 mg (0.47 mmol) of the title compound **21** (47% yield): mp 244–246 °C; IR (KBr) \max 3398 (NH₂), 2191 (CN) cm⁻¹; ¹H-NMR (250 MHz, CDCl₃) δ 8.93–8.91 (m, 1H), 8.22 (dd, *J* = 8.3 Hz, *J* = 1.6 Hz, 1H), 7.59–7.51 (m, 2H), 7.12 (d, *J* = 8.5 Hz, 1H), 6.90–6.84 (m, 4H), 5.83 (s, 1H), 3.56 (s, 3H); ¹³C-NMR (62.9 MHz, CDCl₃) δ 159.4, 148.9, 146.7, 142.3, 136.5, 134.9, 127.1, 125.7, 124.9, 122.6, 121.3, 120.9, 115.8, 117.1, 52.0, 33.9, 31.7. Anal. Calcd. for C₁₇H₁₃N₅O: C, 67.32; H, 4.32; N, 23.09. Found: C, 67.55; H, 4.11; N, 23.25.

*Ethyl 5-amino-2-methyl-4-(1-methyl-1H-imidazol-2-yl)-4,6,7,8-tetrahydrocyclopenta[b]pyranol[3,2-*e*]pyridine-3-carboxylate (1)*. According to the procedure described above, ethyl 6-amino-5-cyano-2-methyl-4-(1-methyl-1H-imidazol-2-yl)-4H-pyran-3-carboxylate (**16**) (290 mg, 1.0 mmol), AlCl₃ (200 mg, 1.53 mmol), and cyclopentanone (130 mg, 1.54 mmol), gave 191 mg (0.54 mmol) of the title compound **1** (54% yield): mp 160–161 °C; IR (KBr) \max 3344 (NH₂); 1704 (CO) cm⁻¹; ¹H-NMR (250 MHz, CDCl₃) δ 6.85 (s, 1H), 6.66 (s, 1H), 5.43 (s, 1H), 5.11 (br s, 2H), 4.14–4.02 (m, 2H), 3.42 (s, 3H), 2.87–2.77 (m, 2H), 2.65–2.59 (m, 2H), 2.47 (s, 3H), 2.05–2.02 (m, 2H), 1.14–2.05 (m, 3H); ¹³C-NMR (62.9 MHz, CDCl₃) δ 166.4, 162.4, 161.3, 155.6, 150.1, 147.0, 126.2, 122.6, 118.1, 101.6, 94.5, 60.4, 34.4, 34.3, 32.9, 27.0, 22.1, 19.3, 14.1. Anal. Calcd. for C₁₉H₂₂N₄O₃: C, 64.39; H, 6.26; N, 15.81. Found: C, 64.16; H, 6.37; N, 15.77.

*Ethyl 5-amino-2-methyl-4-(1-methyl-1H-imidazol-2-yl)-6,7,8,9-tetrahydro-4H-pyranol[2,3-*b*]quinoline-3-carboxylate (2)*. Ethyl 6-amino-5-cyano-2-methyl-4-(1-methyl-1H-imidazol-2-yl)-4H-pyran-3-carboxylate (**16**) (300 mg, 1.04 mmol), cyclohexanone (150 mg, 1.53 equiv), and AlCl₃ (200 mg, 1.53 mmol), gave 272 mg (0.74 mmol) of the title compound **2** (72% yield): mp 222–224 °C; IR (KBr) \max 3343 (NH₂); 1701 (CO) cm⁻¹; ¹H-NMR (250 MHz, CDCl₃) δ 6.86 (s, 1H), 6.67 (s, 1H), 5.42 (s, 1H), 5.15 (br s, 2H), 4.22–3.99 (m, 2H), 3.43 (s, 3H), 2.70–2.68 (m, 2H), 2.49 (s, 3H), 2.35–2.17 (m, 2H), 1.73–1.15 (m, 4H), 1.13–1.10 (m, 3H); ¹³C-NMR (62.9 MHz, CDCl₃) δ 166.5, 161.4, 154.3, 153.4, 152.1, 147.0, 126.2, 122.6, 113.6, 101.7, 94.3,

60.5, 34.5, 33.0, 32.5, 22.8, 22.5, 22.3, 19.4, 14.2. Anal. Calcd. for C₂₀H₂₄N₄O₃: C, 65.20; H, 6.57; N, 15.21. Found: C, 65.41; H, 6.33; N, 15.02.

Ethyl 5-amino-2-methyl-4-(1-methyl-1H-imidazol-2-yl)-4,6,7,8,9,10-hexahydrocyclohepta[b]pyranol[3,2-e]pyridine-3-carboxylate (3). Following the general procedure, ethyl 6-amino-5-cyano-2-methyl-4-(1-methyl-1H-imidazol-2-yl)-4H-pyran-3-carboxylate (**16**) (300 mg, 1.04 mmol), AlCl₃ (200 mg, 1.53 mmol), cycloheptanone (170 mg, 1.51 mmol), gave 295 mg (0.77 mmol) of the title compound **3** (74% yield): mp 196–198 °C; IR (KBr) max 3343 (NH₂); 1701 (CO) cm⁻¹; ¹H-NMR (250 MHz, CDCl₃) δ 6.82 (s, 1H), 6.65 (s, 1H), 5.35 (s, 1H), 5.19 (br s, 2H), 4.16–4.01 (m, 2H), 3.40 (s, 3H), 2.81–2.77 (m, 2H), 2.45–2.40 (m, 5H), 1.79–1.42 (m, 6H), 1.12–1.14 (m, 3H); ¹³C-NMR (62.9 MHz, CDCl₃) δ 166.3, 161.2, 160.8, 152.9, 151.1, 146.8, 126.1, 122.6, 118.8, 101.7, 95.1, 60.3, 38.5, 34.5, 32.9, 32.0, 29.6, 26.6, 26.0, 25.5, 19.2, 14.1. Anal. Calcd. for C₂₁H₂₆N₄O₃: C, 65.95; H, 6.85; N, 14.65. Found: C, 66.01; H, 6.66; N, 14.84.

1-(5-Amino-2-methyl-4-(1-methyl-1H-imidazol-2-yl)-6,7,8,9-tetrahydro-4H-pyranol[2,3-b]quinolin-3-yl)ethan-1-one (4). In accordance with the general procedure, 5-acetyl-2-amino-6-methyl-4-(1-methyl-1H-imidazol-2-yl)-4H-pyran-3-carbonitrile (**17**) (260 mg, 1.0 mmol), cyclohexanone (150 mg, 1.53 mmol), and AlCl₃ (200 mg, 1.53 mmol), gave 175 mg (0.52 mmol) of the title compound **4** (52% yield): mp 243–245 °C; IR (KBr) max 3359 (NH₂); 1689 (CO) cm⁻¹; ¹H-NMR (250 MHz, CDCl₃): δ 6.84 (s, 1H), 6.68 (s, 1H), 5.39 (s, 1H), 5.07 (br s, 2H), 3.37 (s, 3H), 2.65–2.49 (m, 2H), 2.36 (s, 3H), 2.23–2.15 (m, 5H), 1.75–1.67 (m, 4H); ¹³C-NMR (62.9 MHz, CDCl₃) δ 199.1, 159.2, 154.5, 153.2, 151.9, 146.2, 126.3, 123.3, 113.5, 109.4, 93.9, 35.2, 33.0, 32.4, 29.7, 22.7, 22.4, 22.2, 19.6. Anal. Calcd. for C₁₉H₂₂N₄O₂: C, 67.44; H, 6.55; N, 16.56. Found: C, 67.31; H, 6.63; N, 16.44.

11-Amino-7,7-dimethyl-10-(1-methyl-1H-imidazol-2-yl)-2,3,6,7,8,10-hexahydrochromeno[2,3-b]cyclopenta[e]pyridin-9(1H)-one (5). According to the procedure, 2-amino-7,7-dimethyl-4-(1-methyl-1H-imidazol-2-yl)-5-oxo-5,6,7,8-tetrahydro-4H-chromene-3-carbonitrile (**18**) (300 mg, 1.0 mmol), anhydrous AlCl₃ (200 mg, 1.5 mmol) in dry ClCH₂CH₂Cl (10 mL), and cyclopentanone (130 mg, 1.54 mmol) gave 185 mg (0.51 mmol) of the title compound **5** (51% yield): mp > 260 °C; IR (KBr) max 3442 (NH₂), 1643 (CO) cm⁻¹; ¹H-NMR (250 MHz, CDCl₃) δ 6.80 (s, 1H), 6.67 (s, 1H), 5.29 (s, 1H), 4.98 (br s, 2H), 3.41 (s, 3H), 2.60–2.57 (m, 2H), 2.43–2.22 (m, 4H), 2.15–2.06 (m, 2H), 1.96–1.04 (m, 2H), 0.99 (s, 6H); ¹³C-NMR (62.9 MHz, CDCl₃) δ 196.0, 165.7, 162.0, 155.4, 150.2, 146.7, 126.6, 122.0, 118.4, 109.0, 95.4, 50.5, 41.2, 34.0, 32.7, 31.8, 30.3, 28.3, 28.2, 26.9, 22.0. Anal. Calcd. for C₂₁H₂₄N₄O₂: C, 69.21; H, 6.64; N, 15.37. Found: C, 69.01; H, 6.44; N, 15.55.

11-Amino-3,3-dimethyl-12-(1-methyl-1H-imidazol-2-yl)-2,3,4,7,8,9,10,12-octahydro-1H-chromeno[2,3-b]quinolin-1-one (6). Using the same procedure, 2-amino-7,7-dimethyl-4-(1-methyl-1H-imidazol-2-yl)-5-oxo-5,6,7,8-tetrahydro-4H-chromene-3-carbonitrile (**18**) (300 mg, 1.0 mmol), AlCl₃ (200 mg, 1.53 mmol), and cyclohexanone (150 mg, 1.53 mmol), gave 132 mg (0.35 mmol) of the title compound **6** (35% yield): mp > 260 °C; IR (KBr) max 3341 (NH₂); 1702 (CO) cm⁻¹; ¹H-NMR (250 MHz, CDCl₃) δ 6.94 (s, 1H), 6.69 (s, 1H), 5.36 (s, 1H), 4.99 (br s, 2H), 3.49 (s, 3H), 2.75–2.61 (m, 4H), 2.40–2.20 (m, 4H), 1.83–1.31 (m, 4H), 1.14 (s, 6H); ¹³C-NMR (62.9 MHz, CDCl₃) δ 196.3, 166.0, 161.2, 154.4, 152.4, 146.9, 127.1, 122.3, 114.1, 109.4, 95.4, 50.8, 41.6, 33.0, 32.5, 32.2, 30.8, 28.6, 22.9, 22.6, 22.4; Anal. Calcd. for C₂₂H₂₆N₄O₂: C, 69.82; H, 6.92; N, 14.80. Found: C, 69.66; H, 6.78; N, 14.67.

13-(1-Methyl-1H-imidazol-2-yl)-9,10,11,13-tetrahydrobenzo[5,6]chromeno[2,3-b]cyclopenta[e]pyridin-12-amine (7). In accordance with the general procedure, 2-amino-1-(1-methyl-1H-imidazol-2-yl)-1H-benzo[f]chromene-3-carbonitrile (**19**) (300 mg, 1.0 mmol), AlCl₃ (200 mg, 1.53 mmol), cyclopentanone (130 mg, 1.54 mmol), gave 202 mg (0.55 mmol) of the title compound **7** (55% yield): mp > 260 °C; IR (KBr) max 3352 (NH₂) cm⁻¹; ¹H-NMR (250 MHz, CDCl₃) δ 8.20 (d, J = 8.4 Hz, 1H), 7.86–7.82 (m, 2H), 7.50–7.39 (m, 3H), 6.96 (s, 1H), 6.59 (s, 1H), 6.29 (s, 1H), 5.32 (br s, 2H), 3.08 (s, 3H), 2.99–2.91 (m, 2H), 2.77–2.64 (m, 2H), 2.21–2.09 (m, 2H); ¹³C-NMR (62.9 MHz, CDCl₃) δ 162.8, 156.6, 150.6, 149.5, 147.8, 131.7, 130.8, 130.3, 128.5, 127.5, 126.3, 124.7, 123.5, 123.1, 118.0, 117.6, 110.5, 94.7, 34.8, 34.4, 32.9, 27.3, 22.1. Anal. Calcd. for C₂₃H₂₀N₄O: C, 74.98; H, 5.47; N, 15.21. Found: C, 75.01; H, 5.51; N, 15.02.

14-(1-Methyl-1H-imidazol-2-yl)-9,11,12,14-tetrahydro-10H-benzo[5,6]chromeno[2,3-b]quinolin-13-amine (**8**). Following the general procedure, 2-amino-1-(1-methyl-1H-imidazol-2-yl)-1H-benzo[*f*]chromene-3-carbonitrile (**19**) (300 mg, 1.0 mmol), AlCl₃ (200 mg, 1.53 mmol), and cyclohexanone (150 mg, 1.53 mmol), gave 225 mg (0.59 mmol) of the title compound **8** (59% yield): mp > 260 °C; IR (KBr)_{max} 3351 (NH₂) cm⁻¹; ¹H-NMR (250 MHz, CDCl₃) δ 8.20 (d, *J* = 8.3 Hz, 1H), 7.84–7.80 (m, 2H), 7.52–7.37 (m, 3H), 6.94 (s, 1H), 6.56 (s, 1H), 6.25 (s, 1H), 5.37 (br s, 2H), 3.08 (s, 3H), 2.88–2.72 (m, 2H), 2.44–2.26 (m, 2H), 1.85–1.77 (m, 4H); ¹³C-NMR (62.9 MHz, CDCl₃) δ 154.5, 154.4, 152.6, 149.5, 147.6, 131.7, 130.7, 130.3, 128.5, 127.4, 126.1, 124.6, 123.4, 122.9, 118.0, 112.9, 110.5, 94.4, 34.7, 32.8, 32.6, 22.9, 22.7, 22.5. Anal. Calcd. for C₂₄H₂₂N₄O: C, 75.37; H, 5.80; N, 14.65. Found: C, 75.30; H, 5.82; N, 14.38.

15-(1-Methyl-1H-imidazol-2-yl)-9,10,11,12,13,15-hexahydrobenzo[5,6]chromeno[2,3-*b*]cyclohepta[*e*]pyridin-14-amine (**9**). Following the general procedure, 2-amino-1-(1-methyl-1H-imidazol-2-yl)-1H-benzo[*f*]chromene-3-carbonitrile (**19**) 300 mg (1.0 mmol), AlCl₃ (200 mg, 1.53 mmol), and cycloheptanone (170 mg, 1.51 mmol), gave 238 mg (0.6 mmol) of the title compound **9** (60% yield): mp > 260 °C; IR (KBr)_{max} 3355 (NH₂ cm⁻¹); ¹H-NMR (250 MHz, CDCl₃) δ 8.21 (d, *J* = 8.2 Hz, 1H), 7.84–7.80 (m, 2H), 7.52–7.37 (m, 3H), 6.95 (s, 1H), 6.57 (s, 1H), 6.32 (s, 1H), 5.43 (br s, 2H), 3.09 (s, 3H), 2.96–2.92 (m, 2H), 2.57–2.53 (m, 2H), 1.87–1.53 (m, 6H); ¹³C-NMR (62.9 MHz, CDCl₃) δ 161.1, 154.1, 151.7, 149.5, 147.6, 131.7, 130.7, 130.3, 128.5, 127.4, 126.2, 124.6, 123.4, 123.0, 118.3, 117.9, 110.6, 95.4, 38.9, 35.0, 32.8, 32.3, 26.9, 26.2, 25.7. Anal. Calcd. For C₂₅H₂₄N₄O: C, 75.73; H, 6.10; N, 14.13. Found: C, 75.66; H, 6.23; N, 14.01.

7-(1-Methyl-1H-imidazol-2-yl)-9,10,11,12-tetrahydro-7H-benzo[7,8]chromeno[2,3-*b*]quinolin-8-amine (**10**). Following the general procedure, 2-amino-4-(1-methyl-1H-imidazol-2-yl)-4H-benzo[*h*]chromene-3-carbonitrile (**20**) (300 mg, 1.0 mmol), cyclohexanone (150 mg, 1.53 mmol), and AlCl₃ (200 mg, 1.53 mmol), gave 198 mg (0.52 mmol) of the title compound **10** (52% yield): mp > 260 °C; IR (KBr)_{max} 3355 (NH₂) cm⁻¹; ¹H-NMR (250 MHz, CDCl₃) δ 8.27 (d, *J* = 8.3 Hz, 1H), 7.85–7.81 (m, 2H), 7.50–7.40 (m, 3H), 6.95 (s, 1H), 6.58 (s, 1H), 6.26 (s, 1H), 5.32 (br s, 2H), 3.09 (s, 3H), 2.81–2.80 (m, 2H), 2.45–2.25 (m, 2H), 1.86–1.78 (m, 4H); ¹³C-NMR (62.9 MHz, CDCl₃) δ 154.6, 154.5, 152.6, 149.5, 147.7, 131.7, 130.7, 130.3, 128.5, 127.5, 126.1, 124.7, 123.5, 122.9, 118.0, 113.0, 110.6, 94.5, 34.8, 32.8, 32.7, 22.9, 22.7, 22.5. Anal. Calcd. for C₂₄H₂₂N₄O: C, 75.37; H, 5.80; N, 14.65. Found: C, 75.12; H, 5.75; N, 14.58.

7-(1-Methyl-1H-imidazol-2-yl)-7,9,10,11,12,13-hexahydrobenzo[7,8]chromeno[2,3-*b*]cyclohepta[*e*]pyridin-8-amine (**11**). Following the general procedure, 2-amino-4-(1-methyl-1H-imidazol-2-yl)-4H-benzo[*h*]chromene-3-carbonitrile (**20**) (300 mg, 1.0 mmol), cycloheptanone (170 mg, 1.51 mmol), and AlCl₃ (200 mg, 1.53 mmol), gave 245 mg (0.62 mmol) of the title compound **11** (62% yield): mp > 260 °C; IR (KBr)_{max} 3350 (NH₂) cm⁻¹; ¹H-NMR (250 MHz, CDCl₃) δ 8.21 (d, *J* = 8.3 Hz, 1H), 7.84–7.80 (m, 2H), 7.51–7.42 (m, 3H), 6.99 (s, 1H), 6.58 (s, 1H), 6.25 (s, 1H), 5.43 (br s, 2H), 3.00 (s, 3H), 2.96–2.92 (m, 2H), 2.57–2.52 (m, 2H), 1.88–1.27 (m, 6H); ¹³C-NMR (62.9 MHz, CDCl₃) δ 161.1, 154.1, 151.7, 149.5, 147.6, 131.6, 130.7, 130.3, 128.5, 127.4, 126.1, 124.7, 123.4, 123.0, 118.3, 117.9, 110.6, 95.3, 38.9, 34.9, 32.8, 32.3, 26.9, 26.5, 25.7. Anal. Calcd. for C₂₅H₂₄N₄O: C, 75.73; H, 6.10; N, 14.13. Found: C, 75.88; H, 6.02; N, 14.25.

7-(1-Methyl-1H-imidazol-2-yl)-7,9,10,11-tetrahydrocyclopenta[5',6']pyrido[3',2':5,6]pyrano[3,2-*h*]quinolin-8-amine (**12**). In accordance with the general procedure, 2-amino-4-(1-methyl-1H-imidazol-2-yl)-4H-pyrano[3,2-*h*]quinoline-3-carbonitrile (**21**) (1.0 mmol, 300 mg), AlCl₃ (200 mg, 1.5 mmol) and cyclopentanone (130 mg, 1.54 mmol), gave 238 mg (0.65 mmol) of title compound **12** (65% yield): mp > 260 °C; IR (KBr)_{max} 3349 (NH₂) cm⁻¹; ¹H-NMR (250 MHz, CDCl₃) δ 9.00–8.98 (m, 1H), 8.11–8.07 (m, 1H), 7.47–7.44 (m, 2H), 7.34–7.23 (m, 1H), 6.94 (s, 1H), 6.71 (s, 1H), 5.89 (s, 1H), 4.92 (br s, 2H), 3.10 (s, 3H), 2.95–2.87 (m, 2H), 2.70–2.59 (m, 2H), 2.15–2.04 (m, 2H); ¹³C-NMR (62.9 MHz, CDCl₃) δ 163.1, 156.7, 150.4, 150.2, 147.8, 146.1, 138.5, 135.6, 128.6, 126.4, 126.3, 123.3, 122.5, 122.1, 117.5, 116.3, 93.5, 36.9, 34.3, 33.0, 27.1, 22.2. Anal. Calcd. for C₂₂H₁₉N₅O: C, 71.53; H, 5.18; N, 18.96. Found: C, 71.48; H, 5.33; N, 19.01.

7-(1-Methyl-1H-imidazol-2-yl)-7,9,10,11,12,13-hexahydrocyclohepta[5',6']pyrido[3',2':5,6]pyrano[3,2-*h*]quinolin-8-amine (**13**). In accordance with the general procedure, 2-amino-4-(1-methyl-1H-imidazol-2-yl)-4H-

pyrano[3,2-*h*]quinoline-3-carbonitrile (**21**) (300 mg, 1.0 mmol), AlCl₃ (200 mg, 1.5 mmol), and cycloheptanone (170 mg, 1.51 mmol), gave 158 mg (0.40 mmol) of title compound **13** (40% yield): mp 206–207 °C; IR (KBr) ν_{\max} 3429 (NH₂) cm⁻¹; ¹H-NMR (250 MHz, CDCl₃) δ 9.00–8.98 (m, 1H), 8.06–8.03 (m, 1H), 7.43–7.36 (m, 2H), 7.28–7.21 (m, 1H), 6.89 (s, 1H), 6.65 (s, 1H), 5.77 (s, 1H), 4.99 (br s, 2H), 3.04 (s, 3H), 2.90–2.76 (m, 2H), 2.63–2.47 (m, 2H), 1.77–1.46 (m, 6H); ¹³C-NMR (62.9 MHz, CDCl₃) δ 161.5, 153.9, 151.1, 150.3, 147.6, 145.9, 138.3, 135.5, 128.4, 126.4, 126.3, 123.2, 122.3, 122.0, 118.1, 116.4, 94.2, 38.4, 37.1, 32.8, 32.1, 26.8, 26.1, 25.5. Anal. Calcd. for C₂₄H₂₃N₅O: C, 72.52; H, 5.83; N, 17.62. Found: C, 72.67; H, 5.85; N, 17.41.

3.5. In Vitro Toxicity in HepG2 Cells

3.5.1. Cell Culture and Treatment

The human hepatoma HepG2 line cells were purchased from American Type Culture Collection. The cells were cultured in Eagle's Minimum Essential Medium (Ozyme, Montigny-le-Bretonneux, France) supplemented with 10% fetal bovine serum, 1X non-essential amino acids, 100 units/mL penicillin and 10 mg/mL streptomycin (Dutscher, Brumath, France). Cultures were kept under a CO₂/air (5%/95%) humidified atmosphere at 37 °C. Prior to the experiment, cells were seeded in 96-well culture plates at a density of 0.1 × 10⁶ cells per well. After 24 h of incubation, the culture medium was refreshed and 100 μ L of the test compounds or DMSO (0.1%) were added. Compounds were tested at 7 concentrations (1–1000 μ M) in triplicate.

3.5.2. Measurement of Cell Viability

Cell viability, measured as the mitochondrial activity of living cells, was determined by quantitative colorimetric assay with 3-[4,5 dimethylthiazol-2-yl]-2,5-diphenyl-tetrazolium bromide (MTT) [33]. Briefly, after 24 h of treatment, cells were incubated with 50 μ L MTT (0.5 mg/mL, Sigma Aldrich) at 37 °C for 2 h. Plates were centrifuged, MTT was removed and 100 μ L DMSO was distributed per well. The absorbance was read at 570 nm by microplate spectrophotometry. Cell viability was expressed as percentage over controls (DMSO, 0.1%).

3.6. Measurement of the Inhibitory Potency against EeAChE

The inhibitory activity on AChE from *Electrophorus electricus* (type VI-S, Sigma, Milan, Italy), was evaluated spectrophotometrically by the method of Ellman *et al.* [27]. AChE stock solution was prepared by dissolving EeAChE lyophilized powder (Sigma) in 0.1 M phosphate buffer (pH = 8.0) containing 0.1% Triton X-100. Stock solutions of the tested compounds (1 mM) were prepared in MeOH/H₂O 50/50 (*v/v*) and diluted in MeOH/H₂O 50/50 (*v/v*). Five increasing concentrations of each inhibitor were used, able to give an inhibition of the enzymatic activity in the range of 20–80%. The assay solution consisted of a 0.1 M phosphate buffer pH 8.0, with the addition of 340 μ M 5,5'-dithio-bis(2-nitrobenzoic acid), 0.02 unit/mL of EeAChE and 550 μ M of substrate (acetylthiocholine iodide, ATCh). Assay solutions with and without inhibitor were preincubated at 37 °C for 20 min followed by the addition of substrate. Blank solutions containing all components except EeAChE were prepared in parallel to account for the non-enzymatic hydrolysis of the substrate. Initial rate assays were performed at 37 °C with a Jasco V-530 double beam spectrophotometer. The rate of increase in the absorbance at 412 nm was followed for 210 s. The velocity in the presence and absence of inhibitor were compared and % inhibition was calculated. The results were plotted by placing the percentage of inhibition in function of the decimal log of the final inhibitor concentration. Linear regression and IC₅₀ values were calculated using Microcal Origin 3.5 software (Microcal Software, Kiev, Ukraine).

3.7. Measurement of the Inhibitory Potency against eqBuChE

The % inhibitory activity on BuChE from horse serum (lyophilized powder, Sigma-Aldrich), was evaluated spectrophotometrically by the method of Ellman *et al.* [27]. BuChE stock solutions were

first dissolved in 0.1 M phosphate buffer (pH 8.0) and then aliquoted in small vials. Compounds were dissolved in DMSO at 10 mM. The reaction was carried out in a final volume of 3 mL of a 0.1 M phosphate-buffered solution at pH 8.0, containing 5,5'-dithiobis-2-nitrobenzoic acid (DTNB, 2625 μ L, 0.35 mM, final concentration), *eq*BuChE (60 μ L, 0.05 U/mL final concentration), tested compound (3 μ L, 10 μ M, final concentration) and 1% *w/v* Bovine Serum Albumin phosphate-buffered (pH 8.0) solution (BSA, 40 μ L). The inhibition with respect to control without compound was determined by pre-incubating this mixture at rt with each compound for 10 min. After this period, butyrylthiocholine iodide (150 μ L, 0.5 mM final concentration) was added and incubated for 15 min at rt. Then the absorbances were measured at 412 nm in a spectrophotometer plate reader (iEMS Reader MF, Labsystems). % inhibition given by each compound was calculated and data are expressed as mean \pm SEM of at least three different experiments.

3.8. Kinetic Analysis of the Inhibition of *EeAChE* by Compound 8

To obtain estimates of the inhibition mechanism, reciprocal plots of $1/v$ vs. $1/[S]$ were constructed at different concentrations of the substrate acetylthiocholine (0.111–0.557 mM) by using Ellman's method [27] and *EeAChE* (type VI-S, Sigma). Four concentrations of inhibitor were selected for this study: 0.850, 2.124, 3.399, 6.798 μ M. The plots were assessed by a weighted least-squares analysis that assumed the variance of the velocity (v) to be a constant percentage of v for the entire data set. Data analysis was performed with GraphPad Prism 4.03 software (GraphPad Software Inc., San Diego, CA, USA). The determination of the non-competitive inhibition constant K_i value was carried out using Dixon plot, *i.e.*, plotting the apparent $1/v$ vs. inhibitor concentration [I] [34] and confirmed by Cornish-Bowden plot ($[substrate]/v$ vs. [I]) [28].

3.9. Oxygen Radical Absorbance Capacity Assay

The radical scavenging activity of *imidazopyranotacrines* 1–13 was determined by the ORAC-FL method [29,30] using a Varioskan Flash plate reader with built-in injectors (Thermo Scientific). Trolox, 2,2'-azobis(amidinopropane) dihydrochloride (AAPH) and fluorescein (FL) were purchased from Sigma-Aldrich. The reaction was performed at 37 $^{\circ}$ C in 75 mM phosphate buffer (pH = 7.4), and the final volume reaction mixture was 200 μ L. The final concentrations were 1–8 μ M for Trolox and 0.1–1 μ M for the tested compounds. Briefly, in a black 96-well microplate (Nunc), antioxidant (20 μ L) and fluorescein (120 μ L) were incubated for 15 min at 37 $^{\circ}$ C. Then, 2,2'-azobis(amidinopropane) dihydrochloride (60 μ L) was added using the built-in injector. The fluorescence at λ_{em} 535 nm (λ_{exc} = 485 nm) was measured each minute during 60 min. All assays were made in triplicate and at least three different assays were performed for each sample. Antioxidant curves were first normalized to the curve of the blank and then, the area under the fluorescence decay curve (AUC) was calculated as:

$$AUC = 1 + \sum(f_i/f_0) \quad (1)$$

where f_0 is the initial fluorescence reading at 0 min and f_i is the fluorescence value at time i .

The net AUC corresponding to a sample was calculated as follows:

$$\text{Net AUC} = AUC_{\text{antioxidant}} - AUC_{\text{blank}} \quad (2)$$

Regression equations were calculated by plotting the net AUC against the antioxidant concentration. The ORAC value was obtained by dividing the slope of the latter curve by the slope of the Trolox curve obtained in the same assay. ORAC values was expressed as μ mol of Trolox equivalent/ μ mol of *imidazopyranotacrines*. Data are expressed as mean \pm SD.

4. Conclusions

Although the etiology of AD is a matter of debate, a number of biological targets [35] such as inhibition of A β oligomerization and deposition in senile plaques, halting neurofibrillary tangle formation, and inhibition of γ - and β -secretase [36] have been identified and exploited to design new therapies. However, the recent failure in clinical phase III of semagacestat [37], γ -secretase inhibitor, as well as the clinical phases discontinuation of tideglusib [38], a GSK-3 inhibitor targeting tau protein, clearly show that the soundest hypotheses for AD have not yet provided any drug for AD patients cure. Thus, this may be the moment to repurpose old strategies such as the search for non-hepatotoxic tacrines.

In this context, in this article we have reported our most recent endeavors on this topic [19], describing a number of *imidazopyranotacrines*, a new type of tacrine analogues [39–43], as modest and selective *EeAChE* inhibitors showing good antioxidant power. Particularly attractive in this family of compounds is the *imidazopyranotacrine* **4**, which is a modest AChEI, but a potent antioxidant agent, endowed with a very interesting safety profile on HepG2 cells, *i.e.*, showing lack of hepatotoxicity even at very high concentration (1000 μ M). Other tacrine analogues such as **8** and **10** are significantly more potent AChEIs than **4** and show good antioxidant power, but also, unfortunately, higher hepatotoxicity, although compare favorably with tacrine especially at high concentrations (≥ 300 μ M). Kinetic analysis showed that compound **8** is a non-competitive AChEI, a mechanism that we have confirmed by computational chemistry by performing the docking analysis of both enantiomers of compound **8** on AChE. In addition, modeling results showed that the best binding positions for compound **8** on BuChE were clustered rather far from the active site, at the top of the gorge, explaining thus why this compound is a poor *eq*BuChE inhibitor (Supplementary Materials).

We have also calculated the Admission, Distribution, Metabolism, Excretion (ADME) properties of some selected *imidazopyranotacrines*. Thus, about 45 physically significant descriptors and pharmacologically relevant properties of both enantiomers of compounds **2**, **4**, **8** and **10** were predicted and some of the important properties were analyzed. All compounds showed significant values for the properties analyzed and showed drug-like characteristics based on Lipinski's rule of five (see Table S1, Supplementary Materials). Drugs currently used for neurological disorders treatment are generally CNS acting drugs, which show values of MW, Hydrogen Bond (HB) donor, acceptors and rotatable bonds, *etc.*, in general, in a smaller range than non-CNS therapeutics. Thus, factors that are relevant to the success of CNS drugs were analyzed. CNS drugs show values of MW < 450, HB donor < 3, HB acceptors < 7, QPlogPo/w < 5, PSA < 90, number of rotatable bonds < 8 and hydrogen bonds < 8. Thus, the enantiomers of compounds **2**, **4**, **8** and **10** satisfied all the characteristic of CNS acting drugs. The solubility of organic molecules in water has a significant impact on many ADME-related properties. These compounds present solubility values within the limits. The partition coefficient (QPlogPo/w), critical for estimation of absorption within the body, ranged between 2.82 and 4.75. The percentage human oral absorption for the compounds is high, 100%. The most used parameter for Blood Brain (BB) barrier penetration is log BB. The log BB of many prescribed CNS drugs is > -0.5 and compounds with log BB < -1.0 penetrate poorly into the brain, yet some commercial CNS drugs have log BB < -1.0. For compounds **2**, **4**, **8** and **10**, these values lie within the indicated limits of $-3 < \text{QPlogBB} < 1.2$.

In conclusion, some *imidazopyranotacrine* derivatives showing selective modest AChE inhibition, whose pharmacokinetic parameters are within the acceptable range defined for human use, thereby indicating their potential as drug-like molecules and possible brain penetration, have been discovered for the potential treatment of AD.

Supplementary Materials: Supplementary materials can be accessed at: <http://www.mdpi.com/1420-3049/21/4/400/s1>.

Acknowledgments: A.B. thanks MESRES (Ministère de l'Enseignement Supérieur et de la Recherche Scientifique, Algeria) for partial financial support. J.M.-C. thanks Maria do Carmo Carreiras (School of Pharmacy, University of Lisbon, Lisbon, Portugal) for critically reading and correcting the manuscript.

Author Contributions: Housseem Boulebd and Abdelmalek Bouraiou carried out the synthesis and spectra analysis and interpretation. Mourad Chioua took care of the elemental analyses. Helene Martin and Alexandre Bonet performed the hepatotoxicity analyses. Lhassane Ismaili carried out the cholinesterase and ORAC analysis. Manuela Bartolini and Vincenza Andrisano performed the cholinesterase inhibition and kinetic studies. José Marco-Contelles wrote the manuscript. Ignacio Moraleda and Isabel Iriepa performed molecular modeling study. Ali Belfaitah conceived the project and conducted collaborative project with José Marco-Contelles and Lhassane Ismaili (Monitoring, coordination and management), analysis of results and spectra analysis and interpretation (chemistry). All authors contributed to and have approved the final manuscript.

Conflicts of Interest: The authors declare no conflict of interest.

References

1. Soler-López, M.; Badiola, N.; Zanzoni, A.; Aloy, P. Towards Alzheimer's root cause: ECSIT as an integrating hub between oxidative stress, inflammation and mitochondrial dysfunction. Hypothetical role of the adapter protein ECSIT in familial and sporadic Alzheimer's disease pathogenesis. *Bioessays* **2012**, *34*, 532–541. [[CrossRef](#)] [[PubMed](#)]
2. Reitz, C.; Brayne, C.; Mayeux, R. Epidemiology of Alzheimer disease. *Nat. Rev. Neurol.* **2011**, *7*, 137–152. [[CrossRef](#)] [[PubMed](#)]
3. Schneider, L.S.; Mangialasche, F.; Andreassen, N.; Feldman, H.; Giacobini, E.; Jones, R.; Mantua, V.; Mecocci, P.; Pani, L.; Winblad, B.; *et al.* Clinical trials and late-stage drug development for Alzheimer's disease: An appraisal from 1984 to 2014. *J. Intern. Med.* **2014**, *275*, 251–283. [[CrossRef](#)] [[PubMed](#)]
4. Ittner, L.M.; Götz, J. Amyloid- β and tau—a toxic pas de deux in Alzheimer's disease. *Nat. Rev. Neurosci.* **2011**, *12*, 65–72. [[CrossRef](#)] [[PubMed](#)]
5. Ávila, J. Tau phosphorylation and aggregation in Alzheimer's disease pathology. *FEBS Lett.* **2006**, *580*, 2922–2927. [[CrossRef](#)] [[PubMed](#)]
6. Rosini, M.; Simoni, E.; Milelli, A.; Minarini, A.; Melchiorre, C. Oxidative stress in Alzheimer's disease: Are we connecting the dots? *J. Med. Chem.* **2014**, *57*, 2821–2831. [[CrossRef](#)] [[PubMed](#)]
7. Murphy, S.L.; Xu, J.Q.; Kochanek, K.D. *Deaths: Final Data for 2010*; National Center for Health Statistics: Hyattsville, MD, USA, 2013.
8. Chacón, M.A.; Reyes, A.E.; Inestrosa, N.C. Acetylcholinesterase induces neuronal cell loss, astrocyte hypertrophy and behavioral deficits in mammalian hippocampus. *J. Neurochem.* **2003**, *87*, 195–204. [[CrossRef](#)] [[PubMed](#)]
9. Terry, A.V.; Buccafusco, J.J.; Wilson, C. Cognitive dysfunction in neuropsychiatric disorders: selected serotonin receptor subtypes as therapeutic targets. *Behav. Brain Res.* **2008**, *195*, 30–38. [[CrossRef](#)] [[PubMed](#)]
10. Gura, T. Hope in Alzheimer's fight emerges from unexpected places. *Nat. Med.* **2008**, *14*, 894. [[CrossRef](#)] [[PubMed](#)]
11. Racchi, M.; Mazzucchelli, M.; Porrello, E.; Lanni, C.; Govoni, S. Acetylcholinesterase inhibitors: Novel activities of old molecules. *Pharmacol. Res. Off. J. Ital. Pharmacol. Soc.* **2004**, *50*, 441–451.
12. Castro, A.; Martínez, A. Targeting Beta-Amyloid Pathogenesis Through Acetylcholinesterase Inhibitors. *Curr. Pharm. Des.* **2006**, *12*, 4377–4387. [[CrossRef](#)] [[PubMed](#)]
13. Rosini, M. Polypharmacology: The rise of multitarget drugs over combination therapies. *Future Med. Chem.* **2014**, *6*, 485–487. [[CrossRef](#)] [[PubMed](#)]
14. León, R.; García, A.G.; Marco-Contelles, J. Recent advances in the multitarget-directed ligands approach for the treatment of Alzheimer's disease. *Med. Res. Rev.* **2013**, *33*, 139–189. [[CrossRef](#)] [[PubMed](#)]
15. Romero, A.; Cacabelos, R.; Oset-Gasque, M.J.; Samadi, A.; Marco-Contelles, J. Novel tacrine-related drugs as potential candidates for the treatment of Alzheimer's disease. *Bioorg. Med. Chem. Lett.* **2013**, *23*, 1916–1922. [[CrossRef](#)] [[PubMed](#)]
16. Reale, M.; Di Nicola, M.; Velluto, L.; D'Angelo, C.; Costantini, E.; Lahiri, D.K.; Kamal, M.A.; Yu, Q.S.; Greig, N.H. Selective acetyl and butyrylcholinesterase inhibitors reduce amyloid-beta *ex vivo* activation of peripheral chemo-cytokines from Alzheimer's disease subjects: Exploring the cholinergic anti-inflammatory pathway. *Curr. Alzheimer Res.* **2014**, *11*, 608–622. [[CrossRef](#)] [[PubMed](#)]
17. Watkins, P.B.; Zimmerman, H.J.; Knapp, M.J.; Gracon, S.I.; Lewis, K.W. Hepatotoxic effects of tacrine administration in patients with Alzheimer's disease. *JAMA* **1994**, *271*, 992–998. [[CrossRef](#)] [[PubMed](#)]

18. Soukup, O.; Jun, D.; Zdarova-Karasova, J.; Patocka, J.; Musilek, K.; Korabecny, J.; Krusek, J.; Kaniakova, M.; Sepsova, V.; Mandikova, J.; *et al.* A resurrection of 7-MEOTA: A comparison with tacrine. *Curr. Alzheimer Res.* **2013**, *10*, 893–906. [[CrossRef](#)] [[PubMed](#)]
19. Zha, X.; Lamba, D.; Zhang, L.; Lou, Y.; Xu, C.; Kang, D.; Chen, L.; Xu, Y.; Zhang, L.; De Simone, A.; *et al.* Novel tacrine-benzofuran hybrids as potent multitarget-directed ligands for the treatment of Alzheimer's disease: Design, synthesis, biological evaluation, and X-ray crystallography. *J. Med. Chem.* **2016**, *59*, 114–131. [[CrossRef](#)] [[PubMed](#)]
20. Martínez-Grau, A.; Marco, J.L. Friedländer reaction on 2-amino-3-cyano-4H-pyrans: Synthesis of derivatives of 4H-pyran[2,3-*b*]quinoline, new tacrine analogues. *Bioorg. Med. Chem. Lett.* **1997**, *7*, 3165–3170. [[CrossRef](#)]
21. Marco, J.L.; de los Ríos, C.; Carreiras, M.C.; Baños, J.E.; Badía, A.; Vivas, N.M. Synthesis and acetylcholinesterase/butyrylcholinesterase inhibition activity of new tacrine-like analogues. *Bioorg. Med. Chem.* **2001**, *9*, 727–732. [[CrossRef](#)]
22. León, R.; Marco-Contelles, J.; García, A.G.; Villarroya, M. Synthesis, acetylcholinesterase inhibition and neuroprotective activity of new tacrine analogues. *Bioorg. Med. Chem.* **2005**, *13*, 1167–1175. [[CrossRef](#)] [[PubMed](#)]
23. Marco-Contelles, J.; León, R.; López, M.G.; García, A.G.; Villarroya, M. Synthesis and biological evaluation of new 4H-pyrano[2,3-*b*]quinoline derivatives that block acetylcholinesterase and cell calcium signals, and cause neuroprotection against calcium overload and free radicals. *Eur. J. Med. Chem.* **2006**, *41*, 1464–1469. [[CrossRef](#)] [[PubMed](#)]
24. Kaptein, B.; Kellogg, R.M.; van Bolhuis, F. Synthesis, molecular structure, and complexation of 1,4-dihydropyridines containing ligands for intramolecular complexation of metal electrophiles. *Recl. Trav. Chim. Pays-Bas* **1990**, *109*, 388–395. [[CrossRef](#)]
25. Okubo, T.; Yoshikawa, R.; Chaki, S.; Okuyama, S.; Nakazato, A. Design, synthesis and structure-affinity relationships of aryloxyanilide derivatives as novel peripheral benzodiazepine receptor ligands. *Bioorg. Med. Chem.* **2004**, *12*, 423–438. [[CrossRef](#)] [[PubMed](#)]
26. Marco-Contelles, J.; Pérez-Mayoral, E.; Samadi, A.; Carreiras, M.C.; Soriano, E. Recent Advances in the Friedländer Reaction. *Chem. Rev.* **2009**, *109*, 2652–2671. [[CrossRef](#)] [[PubMed](#)]
27. Ellman, G.L.; Courtney, K.D.; Andres, V., Jr.; Featherstone, R.M. A new and rapid colorimetric determination of acetylcholinesterase activity. *Biochem. Pharmacol.* **1961**, *7*, 88–95. [[CrossRef](#)]
28. Fang, L.; Kraus, B.; Lehmann, J.; Heilmann, J.; Zhang, Y.; Decker, M. Design and synthesis of tacrine-ferulic acid hybrids as multi-potent anti-Alzheimer drug candidates. *Bioorg. Med. Chem. Lett.* **2008**, *18*, 2905–2909. [[CrossRef](#)] [[PubMed](#)]
29. Cornish-Bowden, A. A simple graphical method for determining the inhibition constants of mixed, uncompetitive and non-competitive inhibitors (Short Communication). *Biochem. J.* **1974**, *137*, 143–144. [[CrossRef](#)] [[PubMed](#)]
30. Dávalos, A.; Gómez-Cordovés, C.; Bartolomé, B. Extending applicability of the oxygen radical absorbance capacity (ORAC-fluorescein) assay. *J. Agric. Food Chem.* **2004**, *52*, 48–54. [[CrossRef](#)] [[PubMed](#)]
31. O'Brien, P.J.; Irwin, W.; Diaz, D.; Howard-Cofield, E.; Krejsa, C.M.; Slaughter, M.R.; Gao, B.; Kaludercic, N.; Angeline, A.; Bernardi, P.; *et al.* High concordance of drug-induced human hepatotoxicity with *in vitro* cytotoxicity measured in a novel cell-based model using high content screening. *Arch. Toxicol.* **2006**, *80*, 580–604. [[CrossRef](#)] [[PubMed](#)]
32. Schoonen, W.G.E.J.; Westerink, W.M.A.; de Roos, J.A.D.M.; Débiton, E. Cytotoxic effects of 100 reference compounds on Hep G2 and HeLa cells and of 60 compounds on ECC-1 and CHO cells. I mechanistic assays on ROS, glutathione depletion and calcein uptake. *Toxicol. In Vitro* **2005**, *19*, 505–516. [[CrossRef](#)] [[PubMed](#)]
33. Denizot, F.; Lang, R. Rapid colorimetric assay for cell growth and survival. Modifications to the tetrazolium dye procedure giving improved sensitivity and reliability. *J. Immunol. Methods* **1986**, *89*, 271–277. [[CrossRef](#)]
34. Dixon, M.; Webb, E.C. *Enzymes*, 2nd ed.; Longmans, Green and Co.: London, UK, 1964; pp. 54–166.
35. Martínez, A. *Emerging Drugs and Targets for Alzheimer's Disease: Neuronal Plasticity, Neuronal Protection and Other Miscellaneous Strategies*; Royal Society of Chemistry: London, UK, 2010; Volume 2, pp. 1–24.
36. Grill, J.D.; Cummings, J.L. Current therapeutic targets for the treatment of Alzheimer's disease. *Expert Rev. Neurother.* **2010**, *10*, 711–728. [[CrossRef](#)] [[PubMed](#)]
37. Haass, C. Semagacestat's fall: Where next for AD therapies? *Nat. Med.* **2013**, *19*, 1214–1215.

38. Lovestone, S.; Boada, M.; Dubois, B.; Hull, M.; Rinne, J.O.; Huppertz, H.-J.; Calero, M.; Andrés, M.V.; Gómez-Carrillo, B.; León, T.; *et al.* A phase II trial of tideglusib in Alzheimer's disease. *J. Alzheimer's Dis.* **2015**, *45*, 75–88.
39. Benchekroun, M.; Bartolini, M.; Egea, J.; Romero, A.; Soriano, E.; Pudlo, M.; Luzet, V.; Andrisano, V.; Jimeno, M.L.; López, M.G.; *et al.* Novel tacrine-grafted Ugi adducts as multipotent anti-Alzheimer drugs: a synthetic renewal in tacrine-ferulic acid hybrids. *Chem. Med. Chem.* **2015**, *10*, 523–539. [[CrossRef](#)] [[PubMed](#)]
40. Nepovimova, E.; Uliassi, E.; Korabecny, J.; Pena-Altamira, L.E.; Samez, S.; Pesaresi, A.; Garcia, G.E.; Bartolini, M.; Andrisano, V.; Bergamini, C.; *et al.* Multitarget drug design strategy: quinone-tacrine hybrids designed to block amyloid-beta aggregation and to exert anticholinesterase and antioxidant effects. *J. Med. Chem.* **2014**, *57*, 8576–8589. [[CrossRef](#)] [[PubMed](#)]
41. Esquivias-Pérez, M.; Maalej, E.; Romero, A.; Chabchoub, F.; Samadi, A.; Marco-Contelles, J.; Oset-Gasque, M.J. Nontoxic and neuroprotective β -naphthotacrines for Alzheimer's disease. *Chem. Res. Toxicol.* **2013**, *26*, 986–992. [[CrossRef](#)] [[PubMed](#)]
42. Chen, Y.; Sun, J.; Fang, L.; Liu, M.; Peng, S.; Liao, H.; Lehmann, J.; Zhang, Y. Tacrine-ferulic acid-nitric oxide (NO) donor trihybrids as potent, multifunctional acetyl- and butyrylcholinesterase inhibitors. *J. Med. Chem.* **2012**, *55*, 4309–4321. [[CrossRef](#)] [[PubMed](#)]
43. Fernández-Bachiller, M.I.; Pérez, C.; González-Muñoz, G.C.; Conde, S.; López, M.G.; Villarroya, M.; García, A.G.; Rodríguez-Franco, M.I. Novel tacrine-8-hydroxyquinoline hybrids as multifunctional agents for the treatment of Alzheimer's disease, with neuroprotective, cholinergic, antioxidant, and copper-complexing properties. *J. Med. Chem.* **2010**, *53*, 4927–4937. [[CrossRef](#)] [[PubMed](#)]

Sample Availability: Samples of all compounds (1)–(21) are available from the authors.



© 2016 by the authors; licensee MDPI, Basel, Switzerland. This article is an open access article distributed under the terms and conditions of the Creative Commons by Attribution (CC-BY) license (<http://creativecommons.org/licenses/by/4.0/>).